# Appendix

# Appendix A

# Soil profiles description

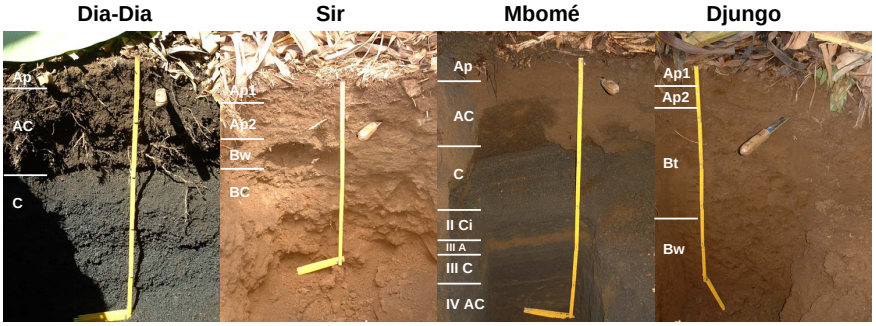


Figure A.1: Mungo weathering sequence from the poorly developped (DD) to the strongly weathered volcanic soil (DJ). Description in Table A.1.

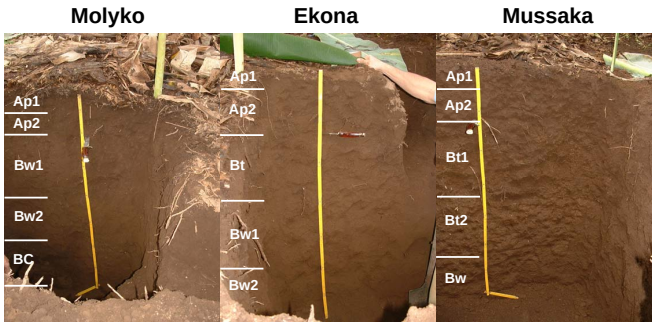


Figure A.2: Mt Cameroon weathering sequence from the poorly developped (MO) to the strongly weathered volcanic soil (MU). Description in Table A.2.

Table A.1: Profiles description (Figure A.1) in the Mungo area.

| **Profile** | **Horiz.** | **Depth (cm)** | **Color *** | **Texture** | **Structure** | **Boundary** |
|---|---|---|---|---|---|---|
| DD | Ap | 0-5 | 10YR2/2 | loam | granular (<cm) | diffuse |
| | AC | 5-40 | 10YR3/2 | loam | granular (cm) | abrupt and wavy |
| | C | 40-100 | 2.5Y2/0 | gravels | scoriae (0.5-3cm) | |
| SR | Ap1 | 0-5 | 10YR2/2 | loam | granular | gradual and regular |
| | Ap2 | 5-21 | 10YR3/1.5 | clay loam | polyhedric subangular (cm) | gradual and regular |
| | Bw | 21-33 | 10YR3/2 | clay to clay loam | polyhedric angular (3cm) | abrupt subhorizontal |
| | BC | 33-80 | 10YR3/4 | clay | polyhedric angular, macroporosity, gravels | indurated slab |
| MB | Ap | 0-5 | 10YR2/2 | clay loam | absent | gradual and regular |
| | AC | 5-32 | 10YR2.5/2 | clay | absent | gradual and regular |
| | C | 32-60 | 10YR2/1 & 7.5YR4/4 | gravels | absent (scoriae) | abrupt and regular |
| | IICi | 60-74 | 10YR2.5/1 | indurated ash | absent | abrupt and regular |
| | IIIA | 74-78 | 10YR3/4 | clay | absent | abrupt and regular |
| | IIIC | 78-95 | 10YR2.5/1 | indurated ash | absent | gradual and regular |
| | IVAC | 95-115 | 10YR3/1 | indurated ash | absent | |
| DJ | Ap1 | 0-5 | 10YR2/1 | clay loam | granular | gradual and regular |
| | Ap2 | 5-15 | 10YR2/2 | clay to clay loam | polyhedric angular (cm) | abrupt and regular |
| | Bt | 15-66 | 10YR3/2 | clay | polyhedric angular (dm) | gradual and regular |
| | Bw | 66-115 | 10YR3/4 | clay to clay loam | polyhedric angular (dm), macroporosity | |

* Munsell colors on dry soil samples

Table A.2: Profiles description (Figure A.2) in the Mt Cameroon area.

| Profile | Horiz. | Depth (cm) | Color * | Texture | Structure | Boundary |
|---|---|---|---|---|---|---|
| MO | Ap1 | 0-5 | 10YR2/1.5 | loam to clay loam | granular | gradual and regular |
| | Ap2 | 5-20 | 10YR2/2 | loam to clay loam | polyhedric subangular (2-5cm) | gradual and regular |
| | Bw1 | 20-60 | 10YR2/2.5 | loam to clay loam | polyhedric angular (2-3cm) | gradual and regular |
| | Bw2 | 60-92 | 10YR3/4 | loam to clay loam | larger, porous | gradual and regular |
| | BC | 92-130 | 10YR3/4.5 | loam to clay loam | gravels | abrupt and wavy |
| | IIA | 130- | 10YR2/1.5 | loam to clay loam | mudflow | |
| EK | Ap1 | 0-5 | 10YR2/1.5 | clay loam to clay | granular | gradual and regular |
| | Ap2 | 5-32 | 10YR2/2 | loam | polyhedric subangular (1-3cm) | gradual and regular |
| | Bt | 32-60 | 10YR3/2 | clay | polyhedric subangular (1-6cm) | gradual and regular |
| | Bw1 | 60-100 | 7.5YR3/2.5 | clay loam | prismatic (10cm) | gradual and regular |
| | Bw2 | 100-140 | 7.5YR3/2.5 | loam | polyangular (3-5cm) | |
| MU | Ap1 | 0-5 | 10YR2/1.5 | clay | polyhedric subangular (1-2cm) | gradual and regular |
| | Ap2 | 5-25 | 10YR2/2 | clay | polyhedric subangular (2-5cm) | gradual and regular |
| | Bt1 | 25-65 | 10YR2.5/2 | clay | polyhedric subangular (2-5cm) | gradual and regular |
| | Bt2 | 65-110 | 7.5YR3.5/2 | clay | prismatic polyangular (10cm) | gradual and regular |
| | Bw | 110-150 | 7.5YR3/2 | clay | polyhedric angular (5-10cm), macroporosity | |

* Munsell colors on dry soil samples

# Appendix B

# GPS coordinates of the sampling sites

Table B.1: GPS coordinates (WGS84) of the sampling sites (soil profiles, irrigation water stations, rivers, parental material).

| **Type** | **Site** | **ID** | **Plot** | **Plantation** | **Latitude N** — degrees minutes — | **Longitude E** — degrees minutes — | **Elevation** m asl |
|---|---|---|---|---|---|---|---|
| Soil profiles | Dia-Dia | DD | DD W04 | PHP | 4.595625 | 9.628794 | 204 |
| | Sir | SR | SI M03 | PHP | 4.619600 | 9.645719 | 240 |
| | Mbomé | MB | MB A17 | PHP | 4.567357 | 9.647547 | 99 |
| | Djungo | DJ | BB Q02 | PHP | 4.608467 | 9.612118 | 163 |
| | Molyko | MO | | CDC | 4.170859 | 9.282215 | 685 |
| | Ekona | EK | | CDC | 4.163581 | 9.293845 | 613 |
| | Mussaka | MU | | CDC | 4.193711 | 9.330061 | 545 |
| Parental material | Mt Pelé | | | | 4.585558 | 9.626775 | 138 |
| Irrigation stations | Dia-Dia lake | | | PHP | 4.592607 | 9.613674 | 136 |
| | Koumbé | | | PHP | 4.587301 | 9.679631 | 106 |
| | Mbomé | | | PHP | 4.568951 | 9.645232 | 85 |
| | Cofruca | | | PHP | 4.573281 | 9.649031 | 79 |
| | Molyko A | | | CDC | 4.173600 | 9.284568 | 668 |
| | Molyko B | | | CDC | 4.167083 | 9.291756 | 628 |
| | Mussaka | | | CDC | 4.190273 | 9.328735 | 495 |
| Rivers | Mungo | | | | 4.144955 | 9.548116 | 16 |
| | Wouri | | | | 4.072523 | 9.697423 | 5 |

# Appendix C

# Preliminary results on intra-plant silicon isotopic fractionation *in situ* vs. *in vitro**


## Abstract

We recently showed that silicon isotopic fractionation in banana (*Musa acuminata* Colla, cv Grande Naine) was related to phytolith production, and therefore to silica content in plant. The present study focuses on isotopic fractionation between the different plant parts. Silicon isotopic compositions were measured using a Nu Plasma multicollector plasma source mass spectrometer (MC-ICP-MS) operating in dry plasma mode. The results are expressed as $\delta^{29}$Si relative to the NBS28 standard, with an average precision and accuracy of ± 0.08‰ (± $2\sigma_{SEM}$). On mature banana (*Musa acuminata* Colla, cv Grande Naine) from Cameroon, $\delta^{29}$Si ranged from +0.13‰ in the petiole to +0.49‰ in the limb, yielding to a 0.36‰ change towards heavier isotopic composition in the upper parts of the plant. This strongly accords with results obtained on *in vitro* banana plantlets cultivated in hydroponics, where the $\delta^{29}$Si increase from pseudostems to limbs is 0.26‰. These preliminary results on *in situ* banana show a trend of intra-plant fractionation comparable with that of *in vitro* hydroponics banana plantlets and with previous data obtained on bamboo.



* Adapted from Opfergelt S., Cardinal, D., Henriet, C., André L., Delvaux, B. (2006) Silicon isotope fractionation between plant parts in banana: *In situ* vs. *in vitro*. *Journal of Geochemical Exploration*, 88, 224-227. www.elsevier.com.

## Introduction

Silicon is absorbed by plants as aqueous $H_4SiO_4$, and precipitates in aerial parts of the plant as biogenic opaline phytoliths. Phytoliths are restored to soils by decomposition of organic debris from plant material. By taking up huge quantities of silica, plants induce a strong biological imprint on silica cycle (Conley, 2002; Derry et al., 2005). The role of higher plants in the biogeochemical cycle of silicon is therefore major (Alexandre et al., 1997) but only a few studies have yet been carried out on silicon isotopic tools to investigate the actual contribution of plants to the silicon continental reservoir (Ding et al., 2003; Douthitt, 1982; Ziegler et al., 2000).

Biomineralization processes are known to fractionate the three stable silicon isotopes ($^{28}Si$, $^{29}Si$, $^{30}Si$) with a preferential uptake of light isotopes (De La Rocha, 2003; De La Rocha et al., 1997).

Just like many other monocotyledons, banana is a Si-accumulator plant (Lahav, 1995). This study concerns *Musa acuminata* Colla, cv Grande Naine. As shown in other crops, silica may enhance plant growth, mineral nutrition, mechanical strength, tolerance to water stress, and resistance to some fungal diseases (Matsuo et al., 1995). We suspect similar effects for banana (unpublished data), an important economical and nutritive resource for many human communities in tropical areas. The mechanisms involved in Si transport into banana remain largely unknown. Recently, we have shown that banana plantlets cultivated in hydroponics fractionate silicon isotopes in a similar extent as other marine organisms (Opfergelt et al. (2006b); Chapter 7). This has important implications on the continental Si isotopic balance (e.g. Basile-Doelsch et al. (2005)). The present study focuses on silicon isotopic fractionation between plant parts in banana cropping system (Cameroon) and compares these preliminary results with previous data obtained from hydroponics.

## Materials and methods

### Area description and sampling (*in situ*)

Banana plant parts (*Musa acuminata* Colla, cv Grande Naine), were collected in January 2004 in Cameroon (Njombé, 70km north of Douala), in a banana collection *in vivo*. In the study area, the rainy season extends from March to November and the total average annual rainfall amounts to 2900 mm $year^{-1}$. Mean annual temperature ranges between 23.5 and 27.5°C. Banana fields are irrigated during the dry season. Soils are

poorly developped volcanic ash soils - Andosol (Delvaux et al., 1989). The international foliar sampling procedure for banana was followed (Martin-Prével, 1984): petiole, central midrib and central limb of leaf III were selected at flowering stage (Figure C.1).

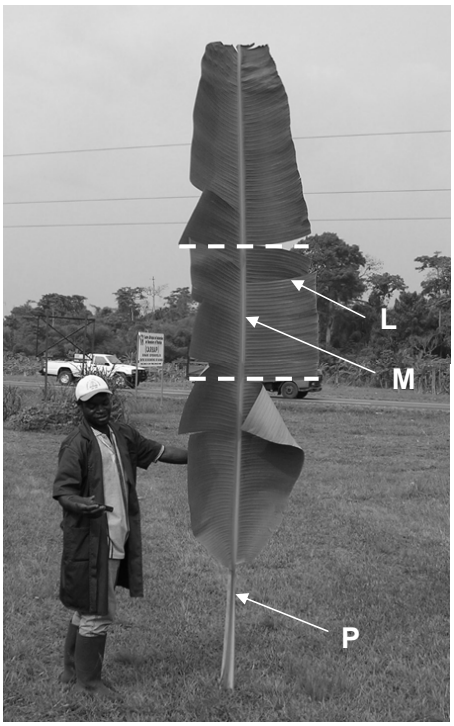


Figure C.1: Foliar samples *in situ* for which the Si isotopic composition and the $SiO_2$ content were measured (P = petiole, M = midrib, L = limb).

## Hydroponics (*in vitro*)

Plantlets of *Musa acuminata* Colla, cv Grande Naine (five replicates) were grown in hydroponics under controlled conditions of light, temperature, humidity and nutrients, during six weeks with a continuous silicon flow of 47 mg $l^{-1}$ Si. Silicon was provided as $H_4SiO_4$, obtained from sodium metasilicate after $Na^+$-$H^+$ exchange by using $H^+$-resin (Amberlite IR120). For each plantlet, three aliquots were made representing three different parts of the plant: pseudostem, midrib and limb (Opfergelt et al., 2004).

### Silica content and Si isotopic analysis

Vegetal samples were dried and crushed. The bulk $SiO_2$ content in various parts of the plant was measured by inductive coupled plasma atomic emission spectrometry (ICP-AES), after borate fusion at 1000°C and dissolution of fusion beads in 10% $HNO_3$.

For isotopic compositions, each separate plant aliquot was processed as described below. Chemical purification consists in: (1) organic matter digestion in hot concentrated suprapur $HNO_3/H_2O_2$ in a 2/1 (v/v) ratio, (2) opal dissolution by 0.2M NaOH leaching at 100°C (Ragueneau et al., 2005), (3) Si purification by TEA-molybdate co-precipitation and combustion in Pt crucibles at 1000°C (De La Rocha et al., 1996), (4) Si dissolution in dilute HF-HCl (Cardinal et al., 2003).

Si isotopic compositions were measured using a Nu Plasma multi-collector plasma source mass spectrometer (MC-ICP-MS), operating in dry plasma mode, and using an external Mg doping to correct mass bias (Cardinal et al., 2003). The results are expressed as $\delta^{29}$Si relative to the NBS28 standard, with an average precision and accuracy of ± 0.08‰ (± $2\sigma_{SEM}$). Presented values are single delta values *in situ* (with standard analytical error bar), and minimum three replicates *in vitro* (with standard deviation).

## Results and discussion

In banana from Cameroon (*in situ*), $\delta^{29}$Si varied between +0.13‰ and +0.49‰ in petioles and limbs, respectively (Figure C.2a). This shows a trend of gradual $\delta^{29}$Si increase of 0.36‰ from petioles to midribs and limbs. This trend towards heavier isotopic compositions in the upper parts of the plant is remarkably similar to the one observed on *in vitro* bananas, even if the $\delta^{29}$Si change from pseudostems to leaves is slightly lower in hydroponics (0.26‰, Chapter 7). Differences between silicon isotopic compositions in banana from Cameroon (+0.13 to +0.49‰) and hydroponics (-0.70 to -0.44‰) are attributed to different isotopic sources signatures. Indeed, hydroponic bananas were supplied by a $H_4SiO_4$ solution with an isotopic composition of -0.02‰ (Opfergelt et al., 2004). No isotopic data are yet available for the Si source in Cameroon but we could expect more positive isotopic signatures as usually observed in continental waters (De La Rocha et al., 2000; Ding et al., 2004). More investigations will be necessary in the future to better constrain the natural source of Si.

Silica content (Figure C.2b) in both natural and hydroponic plants ranged between 0.7 and 4% $SiO_2$, with a large accumulation in the

leaves where the $\delta^{29}$Si is the heaviest. So, there is a positive correlation between silica content and silicon isotopic composition. Moreover, Si contents of *in situ* banana leaves are higher than in hydroponics (4 vs. 3%, respectively). Though the latter were continuously supplied with a solution highly enriched in Si (47 mg $l^{-1}$), this slight difference must be related to the age of the plant (around 10 months *in situ* and 44 days *in vitro*) and to the soil conditions. Banana from Cameroon accumulated silicon during a longer time period and were grown in an Andosol rich in weatherable aluminosilicates (Delvaux et al., 1989).

This general behaviour is comparable to existing data on bamboo by Ding et al. (2003) who showed an increasing $SiO_2$ content (38 to 72%) from stem to branch and leaf, correlated to an increase of isotopic compositions in the plant. However, they measured an increase in $\delta^{29}$Si

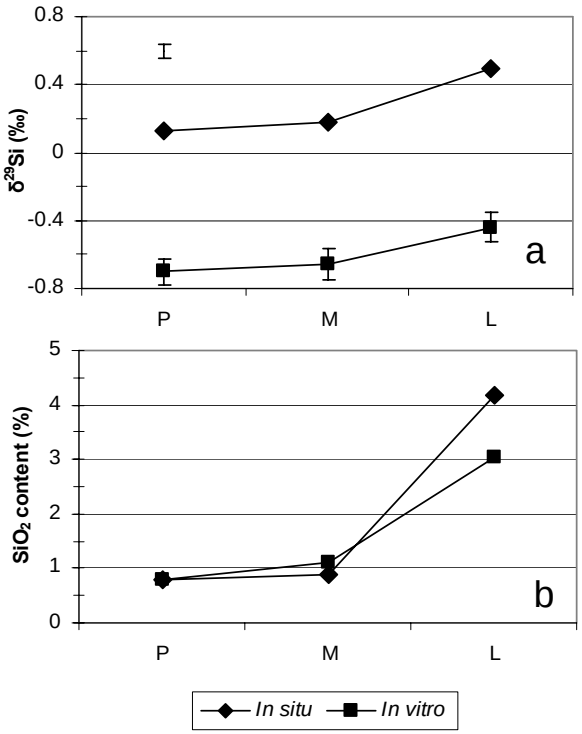


Figure C.2: (a) $\delta^{29}$Si values (‰ vs. NBS28) in banana (P = pseudostem/petiole, M = midrib, L = limb): *in situ* with standard analytical error bar (diamonds) vs. *in vitro* with standard deviation of the replicates (squares). (b) $SiO_2$ content (dry weight %) in banana (P = pseudostem/petiole, M = midrib, L = limb): *in situ* (diamonds) vs. *in vitro* (squares).

ranging from 0.52 to 1.71‰ between different organs within a single stick of bamboo, which is a much larger range than in banana (0.26 to 0.36‰). The twenty-fold higher Si contents in bamboo compared to banana have probably some impact on the isotopic fractionation process within a single plant. This obviously requires further studies of plant species effects on Si isotopic fractionation.

## Conclusions

Here we show that biomineralization of silica in bananas fractionates the stable silicon isotopes in the same extent in natural environment and in hydroponics. The isotopic compositions of the plant phytoliths depend on composition of the source and vary between -0.70 and +0.49‰. Nevertheless the fractionation within a single plant is comparable in both environments and is between 0.26 and 0.36‰. These preliminary results on *in situ* bananas show that even if plants, as other organisms, usually take up preferentially light Si isotopes from the source solution (Opfergelt et al. (2006b); Chapter 7), the intra-plant trend yields to relatively heavier isotopic compositions in upper organs where most of the silica accumulates. This has important implications for the continental Si isotopic balance (e.g. Basile-Doelsch et al. (2005)).

In the future, more investigations will be necessary to have a better constrain on the isotopic composition of the source in natural environments. Thus, we need more data on different varieties of banana. Besides, comparisons have to be done with other Si-accumulating plants.

# Appendix D

# Explore the silicon isotopic variations through banana leaves (Cameroon)

Banana leaves were collected in January 2004 in the worldwide reference *Musa* collection of CARBAP, Cameroon, in two distinct areas: (1) Njombé (elevation: 40-50 m asl), (2) Dschang (highland site: 1400 m asl) (Henriet, 2008). The international foliar sampling procedure for banana was followed (Martin-Prével, 1984): petiole (P), central midrib (M), central internal (IL) and external lamina (EL) of leaf III were selected at flowering stage. The site of Njombé is characterized by an andosol developed on basaltic ash and pumice deposits (Chapter 3), whereas the site of Dschang is constituted by a ferralsol developed from granitic rocks of the base complex (typical red ferralitic soils, Cameroon soil map, Figure 3.9).

Four cultivars with a known Si content (Henriet, 2008) were selected (Njombé) to explore the Si isotopic variations in banana leaves. Among the chosen cultivars, only French Sombre was also available in Dschang for comparison due to distinct adaptation of the genotypes to environmental conditions, especially to elevation.

*Njombé (andosol on basalt)*:
- Grande Naine (genome AAA, subgroup Cavendish)
- Poyo (genome AAA, subgroup Cavendish)
- French Sombre (genome AAB, subgroup Plantain-French)
- Corne Rouge (genome AAB, subgroup Plantain-Faux Corne)

*Dschang (ferralsol on granite)*:
- French Sombre (genome AAB, subgroup Plantain-French)

Table D.1: Si isotopic compositions ($\delta^{29}$Si vs. NBS28, ‰) in banana leaves of four cultivars on two distinct soils (Njombé, Dschang). Leaves parts: P = petiole; M = midrib; IL, EL = internal and external lamina. Cultivars: GN = Grande Naine; PO = Poyo; FS = French Sombre; CR = Corne Rouge.

| Site | Sple ID | $\delta^{29}$Si | $2\sigma_{SD}$ |
|---|---|---|---|
| Njombé | FS P | +0.30 | 0.07 |
| | FS M | -0.01 | 0.08 |
| | FS IL | -0.09 | 0.08 |
| | FS EL | +0.95 | 0.09 |
| | CR P | +0.55 | 0.08 |
| | CR M | +0.18 | 0.10 |
| | CR IL | +0.55 | 0.10 |
| | CR EL | +0.93 | 0.09 |
| | GN P | +0.05 | 0.08 |
| | GN M | -0.05 | 0.08 |
| | GN IL | +0.04 | 0.08 |
| | GN EL | +0.71 | 0.08 |
| | PO P | +0.30 | 0.08 |
| | PO M | +0.06 | 0.08 |
| | PO IL | +0.58 | 0.10 |
| | PO EL | +0.69 | 0.08 |
| Dschang | FS P | +0.72 | 0.09 |
| | FS M | +0.26 | 0.08 |
| | FS IL | +1.01 | 0.10 |
| | FS EL | +1.05 | 0.09 |

The Si isotopic compositions in P, M, IL and EL are presented as $\delta^{29}$Si measured in Table D.1 and as $\delta^{30}$Si calculated in Figure D.1. Few observations can be drawn. A similar trend of heavier isotopic composition in external lamina can be observed, in good agreement with hydoponic and mature banana (Chapter 7 and 8). The large range of isotopic variation displayed by the different cultivars does not indicate any relation with genome (AAA and AAB). However, French Sombre from the ferralitic soil of Dschang displayed a heavier isotopic composition than French Sombre of the andosol of Njombé. As the ferralitic soil of Dschang is much more weathered than the andosol of Njombé, this is in good agreement with the fact that the bulk plant Si isotopic composition might reflect the soil weathering stage (Chapter 8). Moreover, this might suggest an impact of the granitic parental material in Dschang ($\delta^{30}$Si = ∼0.0‰, Ding et al. (1996); Douthitt (1982)) isotopically heavier than the basaltic parental material ($\delta^{30}$Si = -0.38‰, Chapter 12), and should be investigated in more details.

In November 2005, the four leaf parts (P, M, IL and EL) of leaf III, V and VII from *Musa acuminata* Colla, cv Grande Naine were sampled on one plant of the Mussaka station (located in Chapter 3), in order to test the Si content related to ageing leaves (Motomura et al., 2004). The Si content displayed an increasing Si content in all parts from young leaf III to older leaf VII (Figure D.2). As rice and bamboo display larger

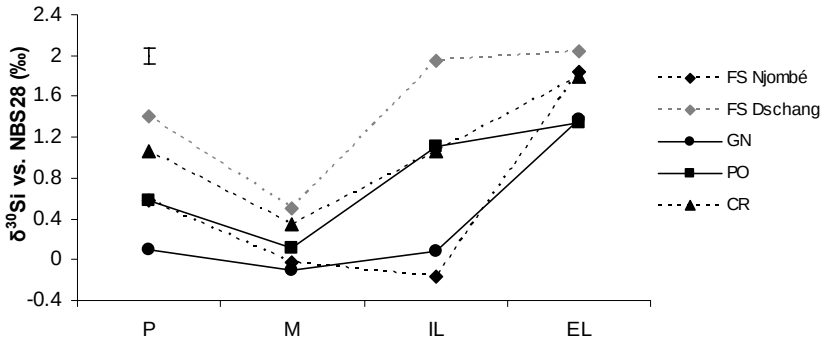


Figure D.1: Si isotopic compositions ($\delta^{30}$Si calculated from $\delta^{29}$Si vs. NBS28, ‰) in banana leaves of four cultivars on two distinct soils (Njombé = black, Dschang = grey). Leaves parts: P = petiole; M = midrib; IL and EL = internal and external lamina. Cultivars: GN = Grande Naine; PO = Poyo; FS = French Sombre; CR = Corne Rouge.

Si isotopic variations (Ding et al., 2005b 2008) and higher Si content than banana, this would be interesting to test the Si isotopic variations among mature banana leaves in relation with their age, and hence with the Si content.

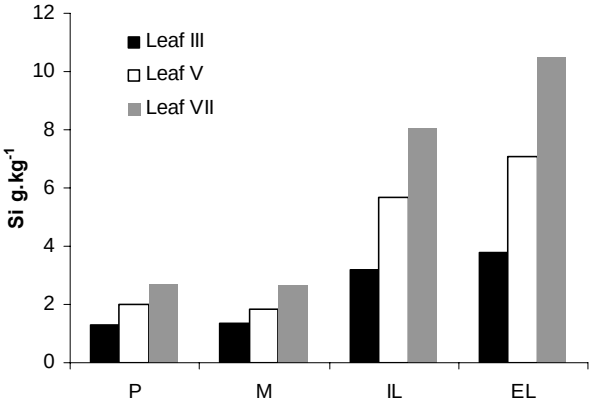


Figure D.2: Evolution of the Si content between leaf III, V and VII in a banana plant from Mussaka site. P = petiole; M = midrib; IL and EL = internal and external lamina.

# Appendix E

# Complementary silicon isotopic compositions in banana

Table E.1: Si isotopic compositions ($\delta^{30}$Si vs. NBS28, ‰) in banana plant (PSi = internal pseudostem; IL = internal limb) in five stations fully described in Chapter 12: SR = Sir, MB = Mbomé; MO = Molyko; EK = Ekona = Mussaka.

| Site | Psi | | IL | |
|---|---|---|---|---|
| | $\delta^{30}$Si | $2\sigma_{SD}$ | $\delta^{30}$Si | $2\sigma_{SD}$ |
| SR | -0.25 | 0.12 | +0.43 | 0.10 |
| MB | +0.32 | 0.12 | +0.65 | 0.10 |
| MO | -0.38 | 0.14 | -0.25 | 0.11 |
| EK | +0.72 | 0.14 | +0.41 | 0.12 |
| MU | +0.57 | 0.13 | -0.14 | 0.11 |

# Appendix F

# Evaluation of the silicon source for adsorption and desorption

## Evaluation of the Si source for $H_4SiO_4^0$ adsorption

In the experiment presented (Chapter 11), we controlled the isotopic signature of the aqueous Si source provided for Si adsorption onto soil Fe-oxides. However, we have shown that soil surfaces were not cleaned and may provide Si by desorption. By using a series of assumptions (further detailed), we propose to compute the Si isotopic signature of the aqueous Si source involved in the adsorption process. The assumptions are following: (1) the Si isotopic fractionation by adsorption is characterized by a stable fractionation factor depending on the Fe-oxide considered (Chapter 10); (2) the Si isotopic fractionation follows a Rayleigh model (Chapter 10); (3) aqueous Si concentration in soil may be also impacted by primary silicate weathering ($\delta^{30}$Si = -0.38‰; Chapter 8), clay formation and dissolution ($\delta^{30}$Si = -1.78 ± 0.83‰; Chapter 8), and biogenic input (mean of +0.33‰; Chapter 8). We are aware of the limit of this calculation as desorption evidenced previously would affect the fractionation factor of pure adsorption used in the calculation.

The Si source considered for monosilicic acid adsorption involves (i) $H_4SiO_4^0$ provided in the ic solution, (ii) the Si pool present on the soil complex and mobile in our experimental conditions. The Rayleigh model predicts the isotopic signature of dissolved Si (DSi) in solution as follows:

$$\delta^{30}Si_{\text{solution}} = \delta^{30}Si_{\text{initial source}} + {}^{30}\varepsilon \ln f \tag{F.1}$$

where $\delta^{30}Si_{solution}$ values were measured in solution (Table 11.5), $f$ is the fraction of Si remaining in solution (Table 11.3), $^{30}\varepsilon$ is the fractionation factor for the adsorption process. We can compute a theoretical fractionation factor $^{30}\varepsilon_{th}$ for each soil material based on the proportion of sro Fe-oxide ($Fe_o/Fe_d$) and crystalline Fe-oxide ($(Fe_d\text{-}Fe_o)/Fe_d$), using the Si isotopic fractionation factor of synthetic ferrihydrite ($^{30}\varepsilon$ = -1.08‰) and goethite ($^{30}\varepsilon$ = -1.60‰) (Chapter 10), which were measured under similar experimental conditions. The values of the theoretical fractionation factor $^{30}\varepsilon_{th}$ are presented in Table F.1. They ranged between -1.10 and -1.51‰ and generally increased with increasing weathering stage.

We can further compute the $\delta^{30}$Si values of the initial Si source from Eq. (F.1). The isotopic signature of the source results from the signatures of the individual sources as computed from each measured $\delta^{30}$Si at each contact time and their corresponding $f$ in solution. The Si source displayed isotopic signatures ($\delta^{30}$Si) ranging from -0.03 to 0.43‰ (Table F.1). The mean $\delta^{30}$Si value in the Mungo sequence was +0.02 ± 0.05‰ at 1.18mMSi, and +0.20 ± 0.05‰ at 0.61mMSi, reflecting the major impact of $H_4SiO_4^0$ provided in the ic solution at 1.18mMSi ($\delta^{30}Si_{ic}$ = +0.02‰ ± 0.07‰). The heavier calculated source at ic = 0.61mMSi (+0.20‰) means that the soil complex Si source of Mungo displayed a positive signature, because of a smaller Si contribution from the experimental initial solution. In Mt Cameroon soils (ic = 1.18mM), the computed value of source $\delta^{30}$Si was +0.26 ± 0.16‰. Relative to Mungo soils, the soil complex Si source should then display a more positive isotopic signature to impact the residual solution.

Contributions to positive isotopic signature for dissolved Si (DSi) in soil originate from irrigation water (+1.19‰; Chapter 12) and biogenic Si from phytoliths (+0.33‰; Chapter 8). The dissolution of primary minerals (unweathered pumice = -0.38‰; Chapter 8), or clay minerals (-1.78 ± 0.83‰; Chapter 8) would give a lighter Si source, which is not in agreement with the calculated source of Si adsorbed. From this calculation (being aware of its limit), we suggest that the Si present onto the soil complex is probably poorly impacted by primary or secondary mineral dissolution. However, soil complex Si source may have been previously impacted by clay formation leaving a heavier residual solution.

Table F.1: Calculated values of $\delta^{30}$Si as computed from Eq. (F.1) to reflect the isotopic composition of the Si source available at the beginning of the batch experiment (Si from experimental solution of given ic and Si from the soil complex). The values of the theoretical fractionation factor ($^{30}\varepsilon_{th}$) were calculated using $^{30}\varepsilon$ of synthetic sro and crystalline Fe oxides (ferrihydrite: -1.08‰; goethite: -1.60‰) (Chapter 10) balanced by the proportion of these minerals.

| Init. mMSi | Profile | $^{30}\varepsilon$ th ‰ | $\delta^{30}$Si source [a] ‰ | mean $\delta^{30}$Si [b] ‰ | st dv [b] ‰ |
|---|---|---|---|---|---|
| 0.61 | DD | -1.10 | +0.17 | | |
| | SR | -1.10 | +0.14 | | |
| | MB | -1.19 | +0.22 | | |
| | DJ | -1.47 | +0.25 | +0.20 | 0.05 |
| 1.18 | DD | -1.10 | -0.03 | | |
| | SR | -1.10 | +0.03 | | |
| | MB | -1.19 | +0.08 | | |
| | DJ | -1.47 | +0.01 | +0.02 | 0.05 |
| 1.18 | MO | -1.32 | +0.13 | | |
| | EK | -1.27 | +0.43 | | |
| | MU | -1.51 | +0.21 | +0.26 | 0.16 |

[a] mean of sources calculated from each mesured $\delta^{30}$Si in solution (Eq.(F.1))

[b] mean and st. dev. of $\delta^{30}$Si source for one experiment

## Contribution of mineral dissolution and Si desorption to the Si isotopic signature

Si desorption from oxide surfaces and Si release from mineral dissolution can be detected during adsorption (e.g. desorption in DD at 24h, Table 11.3 and 11.5; mineral dissolution in MO; see section 11.4.2) or be masked due to a global net Si loss and increase of $\delta^{30}$Si in residual solution. It would be useful to evaluate the proportion of desorption, or in other words, the net adsorption induced. For this purpose, we propose to use isotopic balance calculation to evaluate the proportions of Si released by desorption and/or weathering. This calculation is based on the following assumptions:

(1) Si adsorption follows a Rayleigh model (Chapter 10) with a theoretical fractionation factor $^{30}\varepsilon$ computed for each soil here above (see

Table F.1). Following a modified Eq. (F.1), the additional contribution from desorption (c = $\delta^{30}\mathrm{Si}_{\mathrm{desorp}}$) can be computed as follows:

$$\delta^{30}\mathrm{S}i_{\mathrm{solution}} = \delta^{30}\mathrm{S}i_{\mathrm{initial\ source}} + {}^{30}\varepsilon\ \ln\ f + \mathrm{c} \qquad \text{(F.2)}$$

(2) To be able to compute the proportion of Si provided by desorption, we need to consider that desorption would release Si isotopes adsorbed by a reversible reaction, which has not been demonstrated. To our knowledge, no data are available to support this hypothesis. However, as this is the only way to evaluate the fraction of Si desorbed, we consider this hypothesis to open the reflection. Consequently, desorption would be characterized by an inverse fractionation factor (-$^{30}\varepsilon$). The equation for the desorption process would thus be written as follows:

$$\delta^{30}\mathrm{S}i_{\mathrm{desorb}} = \delta^{30}\mathrm{S}i_{\mathrm{initial\ source}} + (-{}^{30}\varepsilon)\ \ln\ f \qquad \text{(F.3)}$$

where $\delta^{30}\mathrm{Si}_{\mathrm{desorp}}$ is calculated from Eq. (F.2) and $^{30}\varepsilon$ from Table F.1. From Eq. (F.3), the proportion of aqueous Si involved in the desorption process $f$ would be calculated. The Si depletion induced by net Si adsorption was calculated by subtracting Si desorbed from the bulk aqueous Si concentration (Table 11.3). In Figure F.1, the calculated Si concentration left in solution after subtracting the Si desorbed concentration from the bulk aqueous Si concentration, is plotted against Fe-oxide content. Figure F.1 thus considers the net Si adsorption. The calculated Si left in solution readily decreased with increasing $\mathrm{Fe}_d$ content, showing that net Si adsorption increased with increasing Fe-oxide content. MB and EK soil materials were clearly set apart from the general trend, because of their relatively high content of sro Fe-oxide ($\mathrm{Fe}_o/\mathrm{Fe}_d = 0.77$ in MB, and 0.63 in EK), as shown from Si isotopic data (Figure 11.6c). The good agreement of computed data (Figure F.1) with measured isotopic data (Figure 11.6c) supports the interest of this calculation (being aware of its limit). The interpretation of isotopic data thus contributes to ascertain the strong impact of Fe-oxide content and Fe-oxide type on the net adsorption of monosilicic acid in the volcanic ash soils considered here. In other words, the soil weathering stage of these soils, through Fe-oxide content and type, strongly influenced the net adsorption of monosilicic acid and the isotopic signature of the residual solution.

For MO, we further calculated the contribution of Si release from silicate weathering, added to the Si release from oxide surfaces. In this case, the $\delta^{30}\mathrm{Si}_{\mathrm{desorp}}$ of MO (Eq. (F.2)) can be expressed as follows:

$$\delta^{30}Si_{\text{desorb}} = [\delta^{30}Si_{\text{desorb net}} * x] + [\delta^{30}Si_{\text{silicate}} * (1 - x)] \qquad \text{(F.4)}$$

where $x$ corresponds to the Si proportion from desorption, and (1-$x$) to the Si proportion from mineral dissolution. Assuming $\delta^{30}\text{Si}_{\text{desorp net}}$ of MO equal to $\delta^{30}\text{Si}_{\text{desorp}}$ of poorly weathered soils (DD and SR, Eq. (F.2)), and $\delta^{30}\text{Si}_{\text{silicate}}$ of DD at -0.41‰ (Chapter 8), we could estimate the contribution of weathering (1-$x$). This estimation indicates that Si release from oxide surfaces was much similar in MO, SR and DD (not illustrated).

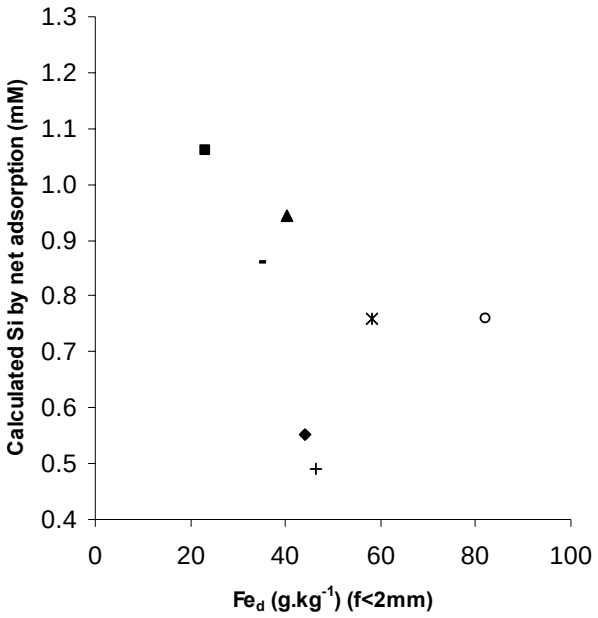


Figure F.1: Si left in solution after 72h contact time (calculated aqueous Si concentration after subtraction of desorbed Si from bulk concentration) vs. $\text{Fe}_d$ content in fine earth fraction, at ic = 1.18mM. DD = square, SR = triangle, MB = diamond, DJ = open circle, MO = dash, EK = cross, MU = star.